DOI 10.5012/bkcs.2011.32.1.325

Axial Interactions of Nitrate Ions to a Silver(II) Ion Supported by C-H···O Hydrogen Bonds in a Silver(II) Tetraazamacrocyclic Complex

Ja Ran Moon, Alan J. Lough, Yong Tae Yoon, Yeong Il Kim, and Ju Chang Kim*

*Department of Chemistry, Pukyong National University, Busan 608-737, Korea. *E-mail: kimjc@pknu.ac.kr*
†Department of Chemistry, University of Toronto, Toronto, ONT, Canada M5S 3H6
Received October 24, 2010, Accepted November 12, 2010

Key Words: Silver(II) complex, Macrocycle, Supramolecule, C-H···O hydrogen bond

Tetraazamacrocycles **L1** and **L2**, first synthesized by Kang *et al*., which are two of the 16 possible diastereoisomers of **L** have long been used for the preparation of many interesting metal complexes.[1-6] Although the macrocycles **L1** and **L2** show similar coordination tendencies to metal ions and form corresponding metal complexes, the chemical and structural properties of metal complexes are greatly influenced by the stereochemistry of cyclohexane rings fused on the 14-membered tetraazamacrocycle. Thus, the axial coordination of solvent molecules to the nickel(II) ion in $[Ni(\mathbf{L1})](ClO_4)_2$ is much easier than that in $[Ni(\mathbf{L2})](ClO_4)_2$.[2] The bicarbonate ligands axially coordinate to the nickel(II) ion in $[Ni(\mathbf{L1})](ClO_4)_2$, but not in $[Ni(\mathbf{L2})](ClO_4)_2$.[3] Two Cp (Cp = cyclopentadienyl) rings of bridging fdc ligands are staggered in $\{[Zn(\mathbf{L1})(fdc)]\cdot 3H_2O\}_n$, but eclipsed in $\{[Zn(\mathbf{L2})(fdc)]\cdot 2H_2O\}_n$ (fdc = 1,1'-ferrocenedicarboxylate ion).[4] The resulting differences between the metal complexes formed with macrocycles **L1** and **L2** in the above examples have been just ascribed to the structural characteristics of the macrocycles **L1** and **L2**. However, it has not been clearly understood what the factors influence to the chemical and structural properties of metal complexes, and explanation and discussions are insufficient to explain the differences between the metal complexes formed with macrocycles **L1** and **L2**. Therefore, we have prepared and studied a silver(II) supramolecular polymer $\{[Ag(\mathbf{L1})](NO_3)_2\cdot 2H_2O\}_n$ (**1**) in order to get further insight into the metal chemistry of **L1**, where the high oxidation state of silver(II) is stabilized by the tetraazamacrocycle **L1** and the axial nitrate ions are supported by the methylene protons of the macrocycle through C-H···O hydrogen bonds. The details of the synthesis, structure, spectroscopic and electrochemical properties of **1** are discussed in this report.

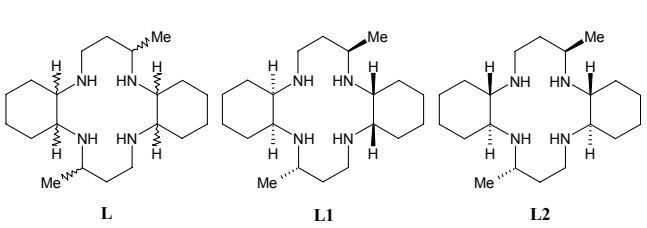

Experimental Section

Materials, Methods and Apparatus. All chemicals used in the synthesis were of reagent grade and used without further purification. Distilled water was used for all procedures. Infrared spectra of solid samples were recorded on a Perkin-Elmer Paragon 1000 FT-IR spectrophotometer between 4000 cm^{-1} and 400 cm^{-1} as Nujol mulls on KBr discs. UV-vis spectra were measured on a Cary 1C spectrophotometer within the range 200 - 800 nm. EPR spectra were obtained by a JES PX2300 digital X-band (ν = 9.453 GHz) spectrometer at ambient temperature. Elemental analysis was performed by the Korea Research Institute of Chemical Technology, Daejeon, Korea. The free ligand **L1** was prepared according to literature procedures.[1] Electrochemical measurements were performed in a standard three electrode system with Pt disk working electrode, $Ag/AgNO_3$ (0.01 M) reference electrode and Pt counter electrode using a PAR 263A potentiostat. The electrolyte solution was 0.1 M triethylammonium hexafluorophosphate (TEAP) in dry acetonitrile. The potential scan rate in cyclic voltammetry was 50 mV s^{-1}. The reference potential of $Ag/AgNO_3$ electrode was 0.045 V *vs*. ferrocene/ferrocenium potential. The concentration of **1** was not determined.

Synthesis of 1. To a methanol (10 mL) solution of **L1** (330 mg, 1.0 mmole) was added a water (10 mL) solution of $AgNO_3$ (680 mg, 2.0 mmole). The mixture turned deep orange and a metallic silver formed immediately. The metallic silver was filtered off. The orange filtrate was collected and allowed in an open beaker protected from light at ambient temperature. The yellow needles of **1** were obtained in a week. Suitable crystals of **1** for X-ray diffraction studies and other measurements were manually collected under a microscope. Yield: 544 mg (90%). mp (dec.) 165 - 167 °C. Anal. Calcd. for $C_{20}H_{44}AgN_6O_8$: C, 39.7; H, 7.3; N, 13.9%. Found C, 39.7; H, 7.4; N, 14.0%. IR (Nujol, cm^{-1}): 3406 (νOH), 3203 (νNH), 1641 (ν_{as} NOO), 1613 (ν_s NOO).

X-ray Crystallography. A summary of selected crystallographic data and structure refinement for **1** is given in Table 1. X-ray data were collected on a Nonius Kappa CCD diffractometer, using graphite monochromated Mo Kα radiation (λ = 0.71073 Å). A combination of 1° ϕ and ω (with κ offsets) scans were used to collect sufficient data. The data frames were integrated and scaled using the Denzo-SMN package.[7] The structure was solved and refined using the SHELXTL\PC V6.1 package.[8] Refinement was performed by full-matrix least squares on F^2 using all data (negative intensities included). Hydrogen atoms other than those of water molecules were included in calculated positions and refined isotropically.

Table 1. Crystal data refinement for **1**

	1
Empirical formula	$C_{20}H_{44}N_6O_8Ag$
Formula weight	604.48
Temperature (K)	150(1)
Wavelength	0.71073 Å
Crystal system	Triclinic
Space group	$P\bar{1}$
Unit cell dimensions	a = 8.5400(4) Å
	b = 8.8773(2) Å
	c = 9.1096(4) Å
	α = 72.838(2)°
	β = 73.2510(18)°
	γ = 77.492(2)°
Volume	625.31(4) Å^3
Z	1
Density (calcd)	1.605 Mg/m^3
Absorption coefficient	0.863 mm^{-1}
Independent reflections	2828 [R(int) = 0.0371]
Goodness-of-fit on F^2	1.079
Final R indices [I > 2σ (I)]	R_1 = 0.0322, wR_2 = 0.0712
R indices (all data)	R_1 = 0.0356, wR_2 = 0.0736

Results and Discussion

The complex **1** was obtained by reacting the macrocycle **L1** and $AgNO_3$ in MeOH/H_2O. The complex **1** exhibits a 1D supramolecular polymer, where the 1D chain is formed by hydrogen bonds between the two sets of pre-organized N-H groups of the macrocycle, nitrate ions and lattice water molecules (Figure 1). Space-filling and lattice diagrams of **1** illustrating the 1D supramolecular chain by hydrogen bonds are described in Figure 2. The coordination environment around the central Ag(II) ion is a square plane with four Ag-N bonds from the macrocycle. The Ag(II) ion sits on an inversion center. Two weak axial interactions for the Ag(II) ion are observed between the Ag(II) ion and the O atoms from nitrate ligands. The Ag-N distances range from Ag1-N1 = 2.1424(18) Å to Ag1-N2 = 2.1788(19) Å. The Ag-O distance of 2.8856(19) Å is long due to Jahn-Teller effect for a d^9 electron configuration and comparable to those of other related complexes ([Ag(**L2**)]$(NO_3)_2{\cdot}4H_2O$; Ag-O = 2.923(2) Å,[9] [Ag(*meso*-**[14]ane**)]$(NO_3)_2$; Ag-O = 2.807(4) Å,[10] [Ag(**tmc**)]$(ClO_4)_2$; Ag-O = 2.889(4),[11] [Ag(**cyclam**)]$(ClO_4)_2$; Ag-O = 2.788(2),[12] where *meso*-**[14]ane** = *meso*-5,5,7,12,12,14-hexamethyl-1,4,8,11-tetraazacyclotetradecane, **tmc** = 1,4,8,11-tetramethyl-1,4,8,11-tetraazacyclotetradecane, **cyclam** = 1,4,8,11-tetraazacyclotetradecane). Two pertinent features are found in the complex **1**. One is that the complex **1** contains the unusual high oxidation state of the Ag(II) ion which is stabilized by the macrocycle **L1**. It has generally been understood that the macrocyclic ligands possessing a suitable cavity size and hard nitrogen donor atoms can form stable Ag(II) complexes in aqueous solution.[13,14] The complex **1** is indefinitely stable in the solid state, but it slowly loses the Ag(II) ion in a prolonged time (~ a month) in DMF solution, giving a metallic silver and a free macrocyclic ligand **L1**. Another noteworthy feature found in **1** is that interactions between the Ag(II) ion and the O atoms of nitrate ions. As stated above, the Ag-O distance of 2.8856(19) Å is long, but it is still shorter than that found in a closely related complex [Ag(**L2**)]$(NO_3)_2{\cdot}4H_2O$.[9] The shorter Ag-O distance in **1** compared to that in [Ag(**L2**)]$(NO_3)_2{\cdot}4H_2O$ can be explained by C-H···O hydrogen bonds {C5-H5B···O3; d = 2.559 Å, D = 3.506 Å, θ = 160.09°, C3-H3B···O1; d = 2.731 Å, D = 3.585 Å, θ = 144.85°}.[15] The D values normally span the range 3.00 -

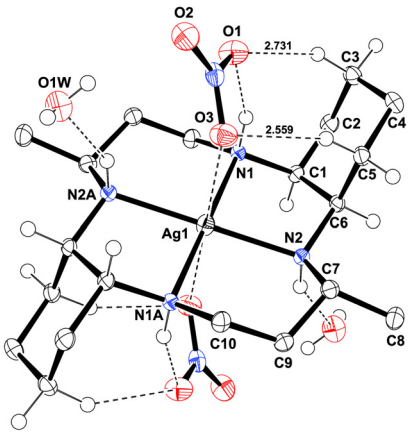

Figure 1. Molecular structure of **1** with atom-labeling scheme. Hydrogen atoms other than those participating in hydrogen bonding and on C1 and C6 are omitted for clarity. Selected interatomic distances (Å) and angles (°): Ag1-N1, 2.1424(18); Ag1-N2, 2.1788(19); Ag1-O3, 2.8856(19); N1-Ag1-N2, 82.44(7); N1-Ag1-N2#1, 97.56(7); N1-Ag1-O3, 86.58(6); N2-Ag1-O3, 97.53(7). Symmetry transformations used to generate equivalent atoms: #1 −x+1, −y+1, −z+1.

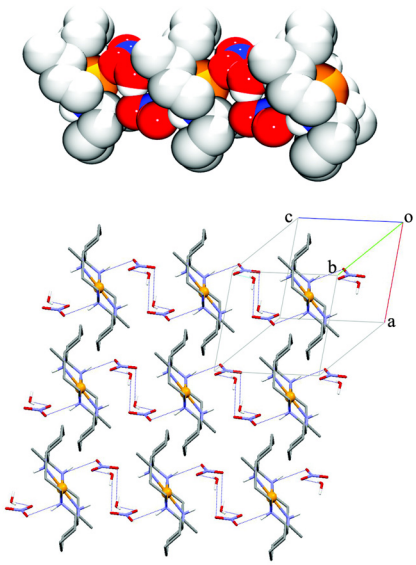

Figure 2. Space-filling (top) and lattice (bottom) diagrams of **1** illustrating a 1D supramolecular chain by hydrogen bonding.

Figure 3. Side view of macrocycles **L1** (left) and **L2** (right).

Table 2. Hydrogen bonds for **1** (Å and °)

D-H···A	d (D-H)	d (H···A)	d (D···A)	< (DHA)
N1-H1···O1	0.93	2.13	2.996(3)	155.1
N2-H2···O1W#1	0.93	2.26	3.113(3)	153.1
O1W-H1WA···O2	0.76(4)	2.15(4)	2.886(3)	164(4)
O1W-H1WB···O3#2	0.72(4)	2.29(4)	2.993(3)	166(4)

Symmetry transformations used to generate equivalent atoms: #1 –x+1, –y+1, –z+1 #2 –x+1, –y+1, –z+2.

4.00 Å with the θ values of a lower limit of 110° while accepting a C-H···O geometry as a hydrogen bond.[15,16] The major structural difference between **1** and [Ag(**L2**)]$(NO_3)_2{\cdot}4H_2O$ is the stereochemistry of the fused cyclohexane rings on the 14-membered tetraazamacrocycle. Thus, the ligand **L1** has two *cis* fused cyclohexane rings that are *anti* with respect to the macrocyclic plane, whereas, the ligand **L2** has two *trans* fused cyclohexane rings that are almost in the same plane with the macrocycle (Figure 3). Under this situation, the presence of C-H···O hydrogen bonds together with the strong N1-H1···O1 hydrogen bond in **1** is believed to stabilize that the nitrate ions interact to the central Ag(II) ion (Figure 1, Table 2). Although even stronger C-H···O hydrogen bond {C10-H10B···O1; d = 2.411 Å, D = 3.361 Å, θ = 163.05°} between one of the hydrogen atoms of the methyl group attached on the 14-membered tetraazamacrocycle and the oxygen atom of the nitrate ion is observed in [Ag(**L2**)]$(NO_3)_2{\cdot}4H_2O$,[9] the possible way of C-H···O hydrogen bond is only one. This implies that the number of possible C-H···O hydrogen bonds play an important role in determining the Ag-O distance, resulting in a shorter distance in **1** than that in [Ag(**L2**)]$(NO_3)_2{\cdot}4H_2O$.

The microanalysis as well as IR and electronic spectra (Figure S1) supported the structure determined by X-ray diffraction studies. The ambient temperature powder EPR spectrum of **1** shows an axial spectrum with principal g-factor values at $g_{\|}$ = 2.10608 and $g_{\perp}$ = 2.02195. The spectrum was typical for a d^9 square planar configuration around the Ag(II) ion (^{107,109}Ag, I = 1/2). The hyperfine structure due to the ^{14}N nuclei (I = 1) was not observed (Figure 4).[13]

The cyclic voltammogram of the complex **1** was quite similar to that observed in [Ag(**L2**)]$(NO_3)_2{\cdot}4H_2O$,[9] but the reduction feature was somewhat different. The successive reduction peaks, A and B in Figure 5 can be assigned to the reduction of $[Ag(\mathbf{L1})]^{2+}$ to $[Ag(\mathbf{L1})]^{+}$ and $[Ag(\mathbf{L1})]^{+}$ to Ag and **L1**, respectively, as described in [Ag(**cyclam**)]$^{2+}$.[17] A clear peak E due to the oxidation of $[Ag(\mathbf{L1})]^{2+}$ to $[Ag(\mathbf{L1})]^{3+}$ appeared at the potential of +0.59 V in the first scan and the corresponding reduction peak was very small relative to the oxidation one. That was decreased in the second scan and stabilized after the second scan. In the case of [Ag(**L2**)]$(NO_3)_2{\cdot}4H_2O$,[9] two separate reductions corresponding to A and B in **1** were not observed in the scan rate of 50 mV/s. This implies that $[Ag(\mathbf{L1})]^{+}$ is more stable than $[Ag(\mathbf{L2})]^{+}$. The oxidation shoulder C can be presumably due to the oxidation of the remaining $[Ag(\mathbf{L1})]^{+}$. The next sharp oxidation peak D is due to the oxidation of deposited Ag to Ag^{+}. Interestingly, the reduction of Ag^{+} to Ag that was observed for [Ag(**L2**)]$(NO_3)_2{\cdot}4H_2O$ was not observed for **1**.

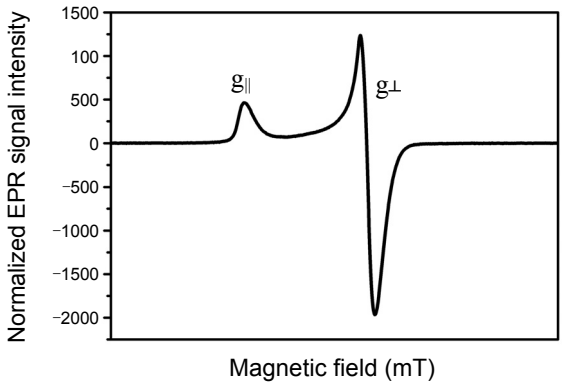

Figure 4. Powder EPR spectrum of **1** at ambient temperature.

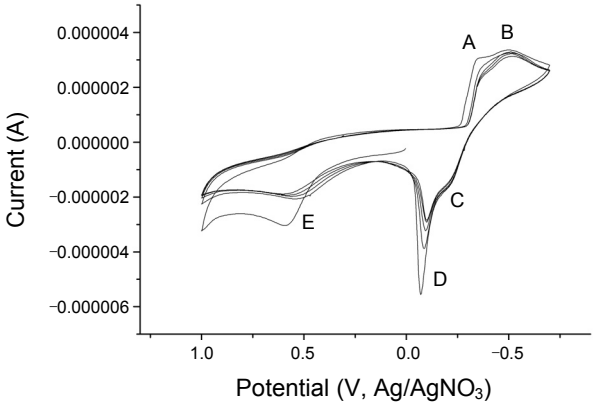

Figure 5. Cyclic voltammogram of **1** in the extended positive potential window between −0.7 and +1.0 V *vs* $Ag/AgNO_3$ (υ = 50 mV s^{-1}, on Pt in 0.1 M TEAP), the concentration of **1** was not determined.

In summary, we have prepared and fully characterized the 1D Ag(II) supramolecule **1** in which the macrocycle **L1** contains the *cis*-fused cyclohexane rings on the 14-membered tetraazamacrocycle. The axial interactions of nitrate ions to the Ag(II) ion are supported by the methylene protons of the macrocycle through C-H···O hydrogen bonds in addition to the N1-H1···O1 hydrogen bond. The electrochemical behavior for **1** indicates that the oxidation of $[Ag(\mathbf{L1})]^{2+}$ is an irreversible process. The electrochemical reduction of $[Ag(\mathbf{L1})]^{2+}$ in **1** indicates that the intermediate $[Ag(\mathbf{L1})]^{+}$ is more stable than $[Ag(\mathbf{L2})]^{+}$ in [Ag(**L2**)]$(NO_3)_2{\cdot}4H_2O$.

Supplementary Material. Crystallographic data have been deposited at the Cambridge Crystallographic Data Center (CCDC), CCDC No. 781801 (**1**). Figure S1 giving IR spectrum in Nujol mull and visible spectrum in methanol for **1**.

References

1. Kang, S.-G.; Kweon, J. K.; Jeong, S.-K. *Bull. Korean Chem. Soc.* **1991**, *12*, 483.
2. Kang, S.-G.; Jeong, J. H. *Bull. Korean Chem. Soc.* **2003**, *24*, 393.
3. Kim, J. C.; Cho, J.; Kim, H.; Lough, A. J. *Chem. Commun.* **2003**, 1796.
4. Kwag, J. S.; Jeong, M. H.; Lough, A. J.; Kim, J. C. *Bull. Korean Chem. Soc.* **2010**, *31*, 2069.

5. Kim, J. A.; Park, H.; Kim, J. C.; Lough, A. J.; Pyun, S. Y.; Roh, J.; Lee, B. M. *Inorg. Chim. Acta* **2008**, *361*, 2087.
6. Park, H.; Kim, J. C.; Lough, A. J.; Lee, B. M. *Inorg. Chem. Commun*. **2007**, *10*, 303.
7. Otwinowski, Z.; Minor, W. In *Methods in Enzymology*, *Macromolecular Crystallography, Part A*; Carter, C. W., Sweet, R. M., Eds.; Academic Press: London, 276 (1997) pp 307-326.
8. Sheldrick, G. M. *SHELXTL\PC V6.1*, Bruker Analytical X-ray Systems, Madison, WI, 2001.
9. Moon, J. R.; Lough, A. J.; Yoon, Y. T.; Kim, Y. I.; Kim, J. C. *Inorg. Chim. Acta* **2010**, *363*, 2682.
10. Mertes, K. B. *Inorg. Chem*. **1978**, *17*, 49.
11. Po, H. N.; Brinkman, E.; Doedens, R. J. *Acta Cryst*. **1991**, *C47*, 2310.
12. Ito, T.; Ito, H.; Toriumi, K. *Chem. Lett*. **1981**, 1101.
13. Ali, M.; Shames, A. I.; Gangopadhyay, S.; Saha, B.; Meyerstein, D. *Transit. Met. Chem*. **2004**, *29*, 463.
14. Sroczyński, D.; Grzejdziak, A. *J. Incl. Phenom. Macrocyclic Chem*. **2002**, *42*, 99.
15. For the definitions of d, D, and θ, see the ref. Desiraju, G. R. *Acc. Chem. Res*. **1996**, *29*, 441.
16. Kuduva, S. S.; Craig, D. C.; Nangia, A.; Desiraju, G. R. *J. Am. Chem. Soc*. **1999**, *121*, 1936.
17. Clark, I. J.; Harrowfield, J. MacB. *Inorg. Chem*. **1984**, *23*, 3740.